

Turbulence of capillary waves revisited

Elena Kartashova[†] and Alexey Kartashov^{*}

[†] *RISC, J. Kepler University, Linz 4040, Austria*

^{*} *AK-Soft, Linz 4030, Austria*

Kinetic regime of capillary wave turbulence is classically regarded in terms of three-wave interactions with the exponent of power energy spectrum being $\nu = -7/4$ (two-dimensional case). We show that a number of assumptions necessary for this regime to occur can not be fulfilled. Four-wave interactions of capillary waves should be taken into account instead, which leads to exponents $\nu = -13/6$ and $\nu = -3/2$ for one- and two-dimensional wavevectors correspondingly. It follows that for general dispersion functions of decay type, three-wave kinetic regime need not prevail and higher order resonances may play a major role.

PACS numbers: 47.35.Pq, 05.45.-a, 47.27.-i

1. Introduction. The very foundations of the kinetic (or statistical) wave turbulence theory have been laid in [19] where kinetic equation for 3-wave interactions of capillary waves has been written out and its stationary solution in the form of power energy spectrum was found.

Kinetic wave turbulence theory is based on a number of assumptions, most important of them being as follows: **I.** weak nonlinearity (nonlinearity is small but non-zero and defined by a small parameter $0 < \varepsilon \ll 1$); **II.** randomness of phases (all waves interact with each other stochastically); **III.** infinite-box limit ($L/\lambda \rightarrow \infty$, where L is the size of the system and λ is characteristic wave length); **IV.** existence of an inertial interval in the wavenumber space (k_0, k_1), where energy input and dissipation are balanced; **V.** locality of interactions in the k -space (only waves with wavelengths of the same order do interact; **VI.** interactions are locally isotropic (no dependence on direction). Under these assumptions, wave kinetic equations have stationary solutions in the form of energy power spectra $E_k \sim k^{-\nu}$, $\nu > 0$, [21].

In the case when dispersion function depends only on one dimensional parameter, say the gravity constant g for water surface gravity waves or surface tension constant σ for capillary waves, one can compute ν using dimensional analysis, without solving the corresponding kinetic equation, [3]. E.g. for a direct cascade we have:

$$\nu = 2\alpha + d - 6 + (5 - 3\alpha - d)/(N - 1), \quad (1)$$

where α is defined by the form of dispersion function $\omega \sim k^\alpha$, d is the space dimension of the system and N is the minimal number of waves constituting a resonance interaction.

It has been first established in the frame of the model of laminated turbulence [7] that energy spectra E_k have gaps formed by exact and quasi-resonances (that is, resonances with small enough resonance broadening). This yields two distinct layers of turbulence in an arbitrary nonlinear wave system – continuous and discrete – and their interplay generates three possible wave turbulence regimes: *kinetic* (energy transport over scales, [21]), *discrete* (dynamical energy exchange within a small finite

set of distinct modes, [8]), and *mesoscopic* (energy transport over scales is already observable although only a finite – fairly big – number of distinct modes should be taken into account, [20]). These regimes and their main features are shown schematically in Fig. 1.

As it was mentioned above, for *kinetic regime* to assumptions **I–VI** must hold, some of which are not easily verified in laboratory. However the advantage in this case is that the knowledge of dispersion function in a wave system immediately yields the explicit form of energy distribution over the scales. On the other hand, the only assumption necessary for *discrete regime* to occur is weak nonlinearity (**I**).

In this Letter we take capillary waves as an illustrative example for showing that the standard approach “decay-type dispersion function \Rightarrow 3-wave kinetic regime” is not universal.

2. Three-wave interactions. Three-wave resonance conditions for capillary water waves with dispersion function $\omega = \sigma k^{3/2}$ read

$$k_1^{3/2} + k_2^{3/2} = k_3^{3/2}, \quad \mathbf{k}_1 + \mathbf{k}_2 = \mathbf{k}_3 \quad (2)$$

Case 1. Wavevectors $\mathbf{k}_j \in \mathbf{Z}^d$ have integer coordinates $\forall j = 1, 2, 3$ (e.g. wave interactions in a resonator are regarded) and d is arbitrary. In this case (2) has no solutions for arbitrary dimension d of the wave vectors, [6].

Case 2. Wavevectors $\mathbf{k}_j \in \mathbf{R}^1$ have real coordinates and $d = 1$. In this case,

$$k_1^{3/2} + k_2^{3/2} = (k_1 + k_2)^{3/2} \Rightarrow k_1 = 0 \text{ or } k_2 = 0, \quad (3)$$

and one can see immediately that for all *positive* \mathbf{k}_j the right hand side of (3) is always greater than its left hand side if both $\mathbf{k}_j \neq 0$. If $k_1 = k$, $k_2 = ck$, with some constant $1 \leq c \leq 10$ (cf. **V**), absolute resonance width

$$\begin{aligned} \Delta_A &= |\omega_1 + \omega_2 - \omega_3| \\ &= |k^{3/2} + c^{3/2}k^{3/2} - [(c+1)k]^{3/2}| \\ &= k^{3/2}|1 + c^{3/2} - (c+1)^{3/2}| > \frac{3\sqrt{c}}{2}k^{3/2} \end{aligned} \quad (4)$$

Layers	Acting elements	Frameworks	Observables	Regimes
discrete	exact and quasi-resonances	infinite k-space	distinct modes, coherent phases	discrete
				mesoscopic
continuous	non-resonant (or approximate) interactions	finite inertial interval In k-space	power spectra of energy, stochastic phases	kinetic

FIG. 1: Schematic representation of wave turbulent regimes.

is rapidly growing function of k when $k \rightarrow \infty$ (cf. **III**). In particular, if $k_1 = k_2 = k$, $\Delta_A \approx 0.82k^{3/2}$.

Case 3. Wavevectors $\mathbf{k}_j \in \mathbf{R}^2$ have real coordinates, $d = 2$, and all three wavevectors are collinear. This case can obviously be reduced to the previous one by an appropriate rotation of coordinate axes.

Case 4. Wavevectors $\mathbf{k}_j \in \mathbf{R}^2$ are real valued and non-collinear. One might argue that if in this case a great amount of *almost collinear* wavevectors form approximate triads with *small resonance width*, we still can expect manifestation of 3-wave kinetic regime in laboratory experiments in the form of power energy spectra $E_{k,3} \sim k^{-7/4}$. This case has been studied numerically and the results are as follows.

2.1. Resonance width. Absolute resonance width Δ_A explicitly depends on \mathbf{k}_1 and considering if it is “small” or “large” the value of k_1 should, of course, be taken into account. It is intuitively clear that for larger vectors larger resonance width is tolerable, and vice versa. Relative resonance width Δ_R , allowing to distinguish between various wave turbulent regimes, might be introduced in a number of ways, e.g. [8, 20] and others; the problems with introducing a general cumulative function Δ_R are discussed in [9], Ch.6.

To perform numerical study of solutions of (2), for a pair of two-dimensional wave vectors $k_1 = (m_1, n_1)$, $k_2 = (m_2, n_2)$ we define relative resonance width as absolute resonance of proportional pair with norm 1, understanding by the norm of a pair of two-dimensional vectors that of the corresponding vector in \mathbf{R}^4 : $\|(k_1, k_2)\| = \sqrt{m_1^2 + n_1^2 + m_2^2 + n_2^2}$ so that

$$\Delta_R = |((\tilde{m}_1^2 + \tilde{n}_1^2)^{3/4} + (\tilde{m}_2^2 + \tilde{n}_2^2)^{3/4} - ((\tilde{m}_1 + \tilde{m}_2)^2 + (\tilde{n}_1 + \tilde{n}_2)^2)^{3/4})| \quad (5)$$

where $\tilde{m}_j = m_j / \|(k_1, k_2)\|$ and $\tilde{n}_j = n_j / \|(k_1, k_2)\|$ with $j = 1, 2$.

2.2. Wavenumbers, norms and angles. Our first series of numerical simulations served to cast a first glance at distribution of wavevectors satisfying (2) in the k -space, primarily, if they are distributed evenly over

the computation domain or concentrated in some restricted subdomains. Calculations were performed on \mathbf{Z}^d grid fragments $-50 \leq m_1, n_1, m_2, n_2 \leq 50$ or $0 \leq m_1, n_1, m_2, n_2 \leq 100$.

Exact resonances (with $\Delta_R = 0$) are achieved for pairs $(k_1, 0)$ and $(0, k_2)$ only (cf. *Case 1*), while for all other pairs (k_1, k_2) approximate interactions may take place. In the Fig.2, left panel, all wavevectors $\mathbf{k}_1, \mathbf{k}_2$ with *non-negative coordinates* taking part in approximate interactions are shown, and their distribution appears to be fairly even. However, if one of the wavevectors, say \mathbf{k}_1 , has non-negative coordinates, all \mathbf{k}_2 interacting with such (middle panel), are distributed in k -space quite irregularly, leaving completely empty the third quadrant and the most part of the first quadrant. Irregularity becomes even more striking if we consider interacting pairs where *both* $\mathbf{k}_1, \mathbf{k}_2$ have non-negative coordinates (right panel). The most part of the domain consists of wavevectors *not participating* in interactions, while interacting vectors are contained in narrow triangles along the axes. Moreover, a simple check shows that wavevectors from the lower triangle interact only with vectors from the upper triangle and vice versa. are shown in the Fig.2, left panel.

To characterize the ratios of norms of interacting vectors (cf. **V**) and angles between them (cf. **VI**), for each solution we computed the ratio of the vector norms k_1/k_2 and the corresponding angle $\widehat{(k_1, k_2)}$ (see Fig.3). It can be seen immediately that solution set is highly anisotropic – angles between interacting wavevectors all belong to the narrow band between 75° and 87° , i.e. interacting wavevectors are almost perpendicular. Norms of the interacting wavevectors can differ by more than 2 orders (Fig.3, left panel) – maximal ratio found in our solution set is $k_1/k_2 = 101.8$. For more than 10% of all the solutions, $k_1/k_2 > 10$. Restriction of our attention to interactions of wavevectors with norms of the same order makes angle anisotropy even more pronounced (Fig.3, right panel) – all angles now lie between 75° and 81° , i.e. the band width becomes twice smaller. Standard averaging by angles spectra, [20], obviously can not give any

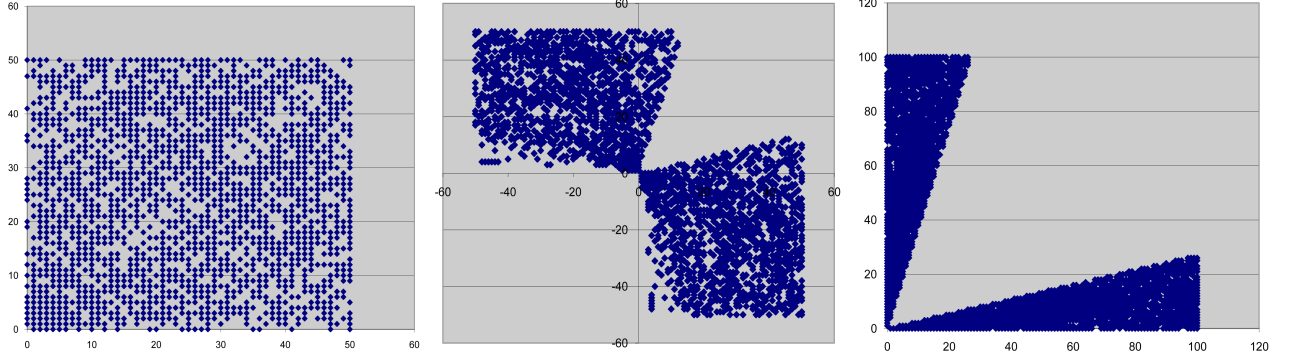


FIG. 2: Two-dimensional wavevectors $\mathbf{k}_1, \mathbf{k}_2$ satisfying (2). **Left panel:** Wavevectors with non-negative coordinates which interact with vectors with arbitrary (positive or negative) coordinates. Computation domain $-50 \leq m_1, n_1 \leq 50$. **Middle panel:** All wavevectors interacting with those shown in the previous panel. Same computation domain. **Right panel:** Both wavevectors have non-negative coordinates. Computation domain $0 \leq m_1, n_1 \leq 100$. Wavevectors from the lower triangle interact only with vectors from the upper triangle and vice versa.

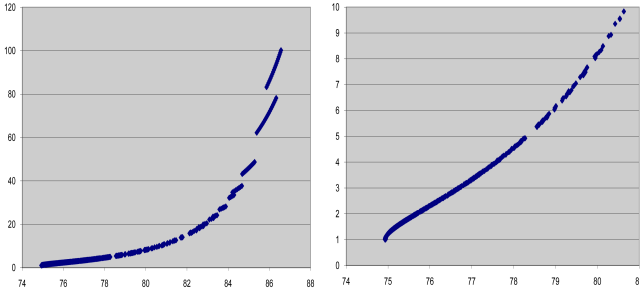


FIG. 3: Dependence of ratio of interacting vectors' norms (longer to shorter) on the angle between vectors. **Left panel:** Complete picture in computation domain $0 \leq m_j, n_j \leq 100$. **Right panel:** Zoomed presentation of the initial interval (ratio ≤ 10) of the left panel. Axes X and Y denote angles (in grad) and ratios correspondingly.

reliable information in this case.

2.3. Resonance curves. Solution distribution irregularities demonstrated above have an elegant explanation. Indeed, let us notice two simple properties of the resonance set of wavevectors satisfying (2):

- if a pair (k_1, k_2) is a solution, then every (ck_1, ck_2) is also a solution for any $c \in \mathbb{R}$
- if a pair (k_1, k_2) is a solution, then every rotated pair $(\mathbf{T}k_1, \mathbf{T}k_2)$ is also a solution for any $\mathbf{T} \in \text{SO}(2, \mathbb{R})$

Therefore, it is enough to compute all vectors k_2 producing resonant interactions with some given \mathbf{k}_1 , say $\mathbf{k}_1 = (0, 1)$ to obtain a clear view of the whole resonant interaction set. Indeed, all resonance partners of $\mathbf{k}_1 = (0, 1)$ constitute a smooth curve shown in Fig. 4. This curve, as a function $n(m)$, starts with a flat region $n \sim m^{3/2}$ (left panel), then becomes steeper and for $m \rightarrow \infty$ has asymptotic $n \sim m^{1/2}$ (right panel). Notice

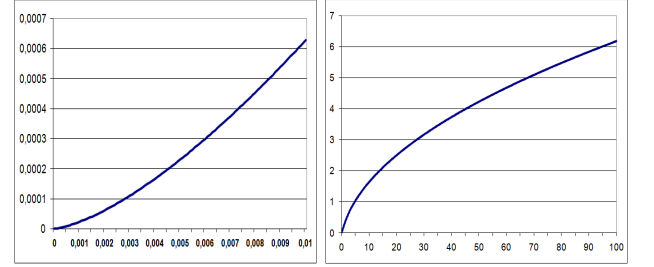


FIG. 4: Color online. Resonance curve of vector $(0, 1)$ in k -space, for dispersion function $\omega \sim k^{3/2}$. **Left panel:** The initial segment of the curve: $m \ll 1 \Rightarrow n \sim m^{3/2}$. **Right panel:** The overall view of the curve: for $m \gg 1 \Rightarrow n \sim m^{1/2}$.

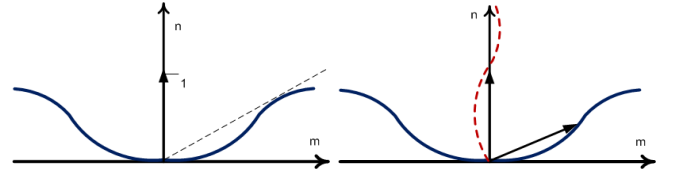


FIG. 5: Color online. Resonance curves in k -space (schematic representation). **Left panel:** For the vector $k_1 = (0, 1)$ all vectors k_2 lie on the interaction curve shown. **Right panel:** Two interacting vectors lie on each other's resonance curves reciprocally. Resonance curve of the rotated vector is shown by the dashed line.

that the two asymptotic regions lie a few magnitudes of 10 apart and can not be illustratively presented in one figure; so we proceed with schematic representation (Fig. 5).

The tangent to the curve drawn from $(0, 0)$ gives the \mathbf{k}_2 with the minimal angle $(\widehat{\mathbf{k}_1 \mathbf{k}_2}) \sim 74.9$. We also see that the unit vector can interact both with vectors of arbitrarily small and arbitrarily large norms k_2 . Notice

that both for $k_2 \rightarrow 0$ and $k_2 \rightarrow \infty$ the angle $(\widehat{\mathbf{k}_1 \mathbf{k}_2}) \rightarrow \pi/2$. Now, any vector $\mathbf{k} \in \mathbb{R}$ can be produced by stretch and rotation of our unit vector, and its resonance curve is obtained by stretching the curve of the unit vector (with the same coefficient) and rotation (by the same angle). If two vectors interact resonantly, then each of them lies on the resonance curve of another (Fig. 5, right panel).

We may conclude with confidence that conditions for 3-wave kinetic regime to occur are decidedly violated. This means that energy cascades observable in various laboratory experiments must have another phenomenology.

3. Dynamic energy cascade. A novel model of a *dynamic energy cascade* generation has been proposed in [9] and is based on resonance clusters of a special form which are due to decay instability. Below we present briefly this model and show how to apply it to capillary waves.

The phenomenon of decay instability has been encountered in various fields and is known under different names – parametric instability in classical mechanics, Suhl instability of spin waves, Oraevsky-Sagdeev decay instability of plasma waves, modulation instability in nonlinear optics, Benjamin-Feir instability in deep water, etc., [12]. All these so very different physical systems can be described in the same frame using the notion of 3-wave interactions

$$\omega_1 + \omega_2 = \omega_3, \quad \mathbf{k}_1 + \mathbf{k}_2 = \mathbf{k}_3, \quad (6)$$

or 4-wave interactions

$$\omega_1 + \omega_2 = \omega_3 + \omega_4, \quad \mathbf{k}_1 + \mathbf{k}_2 = \mathbf{k}_3 + \mathbf{k}_4, \quad (7)$$

where notation $\omega_j = \omega(\mathbf{k}_j)$ is used. For instance, Benjamin-Feir and modulation instabilities are described by (7) with

$$\omega_1 = \omega_3 + \Delta\omega, \quad \omega_2 = \omega_3 - \Delta\omega, \quad (8)$$

where $0 < \Delta\omega \ll 1$,

$$\mathbf{k}_1 + \mathbf{k}_2 = 2\mathbf{k}_3, \quad \omega_1 + \omega_2 = 2\omega_3, \quad (9)$$

parametric instability is governed by (6) with $\mathbf{k}_3 = 0$ which yields $\mathbf{k}_1 = -\mathbf{k}_2$, $\omega_3 = 2\omega_1$ and so on. Notice that parametric instability is usually interpreted via the Mathieu equation, [11], describing the motion of an elastic pendulum when initially the spring-like motion dominates the pendulum-like behavior. However, the modulation equations of motion for an elastic pendulum in three-dimensional space with coordinates x, y, z coincide with the dynamical equations for a resonant triad (6), e.g. [9].

General criterion of the decay instability formulated by Hasselmann in [5] reads as follows. *In a 3-wave system* ω_3 -mode is unstable, if any infinitesimally small excitation of it generates two new modes according to (6);

modes with frequencies ω_1 and ω_2 are neutrally stable. Further on we use notions of A- and P-modes for unstable and stable modes correspondingly (A is for active and P - for passive) as in [10]. (In plasma physics they are sometimes called mother and daughter modes, e.g. [17].) *In a 4-wave system* any one mode is neutrally stable. However, a quartet of the form (9) (called Phillips quartets) “imitates” a triad with A-mode having frequency $2\omega_3$. Energy percolation within a cluster of triads or Phillips quartets can be explained in terms of AA-, AP- and PP-connections within a cluster of arbitrary structure, e.g. [9, 10].

Suppose that in a wave system A-mode is initially excited, then two P-modes are generated. If one of these P-modes happens to be A-mode in another triad or Phillips quartet - two new P-modes will be generated, etc. This process will generate a sequence of nonlinear modes with frequencies

$$\begin{cases} \omega_{1,1} + \omega_{2,1} = \alpha \cdot \omega_{3,1}, \\ \omega_{1,2} + \omega_{2,2} = \alpha \cdot \omega_{3,2}, & \omega_{2,2} = \alpha \cdot \omega_{3,1}, \\ \omega_{1,3} + \omega_{2,3} = \alpha \cdot \omega_{3,3}, & \omega_{2,3} = \alpha \cdot \omega_{3,2}, \\ \dots \\ \omega_{1,n} + \omega_{2,n} = \alpha \cdot \omega_{3,n}, & \omega_{2,n} = \alpha \cdot \omega_{3,(n-1)}, \end{cases} \quad (10)$$

where $\alpha = 1$ in a 3-wave system and $\alpha = 2$ in a 4-wave system. A simple assumption that at each step the same part p of the energy E_0 of the excited A-mode, say pE_0 , $0 < p < 1$, is transferred to the P-mode providing connection with the next triad or Phillips quartet, immediately gives the energy spectrum for the dynamic cascade of the form

$$E_n = p^n E_0, \quad \text{with some constant } 0 < p < 1. \quad (11)$$

If the part of energy p_j varies from step to step,

$$E_n = (\prod_{j=1}^n p_j) E_0, \quad 0 < p_j < 1, \forall j = 1, 2, \dots, n. \quad (12)$$

The number of modes in the dynamic cascade depends on the energy E_0 of the initially excited mode. The process “dies” when the energy of P-modes become too small for weakly nonlinear processes to start, i.e. **IV**. is violated. This means in particular that for smaller E_0 , cascade dies out faster. For bigger E_0 , dynamical cascade is formed only at some initial stage after which periodic or chaotic energy exchange among all modes within a cluster will be observed, though phases are always coherent, see e.g. [2].

Dissipation can also be included in (11) as follows:

$$E_n = (\prod_{j=1}^n \mu_j p^j) E_0 \quad \text{or} \quad (\prod_{j=1}^n \mu_j p_j^j) E_0, \quad (13)$$

where $0 < \mu_j < 1$, $\forall j = 1, 2, \dots, n$, and $\mu_j E_j$ is the part of energy which is lost due to dissipation at the j -th step of the dynamic cascade.

If initially A-mode with frequency $\alpha \cdot \omega_{3,n}$ is excited and all P-modes in (10) have non-zero frequencies, an inverse dynamic cascade is generated:

$$\alpha \cdot \omega_{3,n} > \alpha \cdot \omega_{3,(n-1)} > \dots > \alpha \cdot \omega_{3,1}, \quad (14)$$

while at each cascade step an *A-mode decays into two P-modes*.

Now suppose that at the initial step of excitation of the A-mode with frequency $\omega_{3,1}$, a narrow zero-frequency band $0 < \Delta\omega_0 \ll 1$ – gains some non-zero energy as observed in laboratory experiments, e.g. [13, 16]). Then second harmonic $\omega_{3,1}/2$ is generated via 4-wave interactions of the form $\omega_{1,1} = \omega_{3,1}/2 - \Delta\omega_0$, $\omega_{2,1} = \omega_{3,1}/2 + \Delta\omega_0$. As soon as we have two excited modes, a 3- or 4-wave process may begin in which *two P-modes generate an A-mode*.

In particular, for the case of vertical parametric excitation of capillary waves, cascading cluster (10) takes the form

$$\begin{cases} \omega_{3,1}/2 + \omega_{3,1}/2 = \omega_{3,1}, \\ \omega_{3,1}/2 + \omega_{3,1} = 3\omega_{3,1}/2, \\ \omega_{3,1}/2 + 3\omega_{3,1}/2 = 2\omega_{3,1}, \\ \dots \end{cases} \quad (15)$$

with $\omega_{1,j} = \omega_{3,1}/2$, $\forall j = 1, 2, \dots, n$, and generates a direct dynamic cascade:

$$\omega_{3,1} < 3\omega_{3,1}/2 < 2\omega_{3,1} < \dots < n \cdot \omega_{3,1}/2. \quad (16)$$

Summarizing, initial excitation of *one mode* with frequency ω_{exit} generates an inverse dynamic cascade while zero-frequency mode with non-zero energy "triggers" a direct dynamic cascade. In the later case, 3- and 4-wave interactions of capillary waves take place simultaneously. Both types of interactions are characterized by coherent phases due to the resonance conditions (6) and (7).

Indeed, the evidence of strong four-wave coupling in nonlinear capillary waves has been identified in [16] by computing tricoherence as

$$\tau^2 = |\langle F_1 F_2 F_3 F_{1+2-3}^* \rangle|^2 / \langle |F_1 F_2 F_3|^2 \rangle \langle |F_{1+2-3}|^2 \rangle, \quad (17)$$

where F_j is the Fourier component of the surface elevation at the frequency ω_j . In general, tricoherence τ^2 can change from 0 (no phase coupling) to 1 (coherent phases); in experiments reported in [16] the level of tricoherence $\tau^2 > 0.5$ has been observed.

4. Kinetic cascade vs dynamic cascade. For comparing energy spectra E_k and E_n , it is convenient to rewrite E_n as $E_n = b^{-n} E_0$ with $b = 1/p$, $b > 1$. Thus we have to compare functions $\gamma_1 \cdot b^{-x}$ and $\gamma_2 \cdot x^{-a}$, where the magnitudes of parameters a, b, γ_1, γ_2 are defined by the specific wavesystem. As for $a, b > 1$

$$\lim_{x \rightarrow \infty} (x^a / b^x) = 0, \quad (18)$$

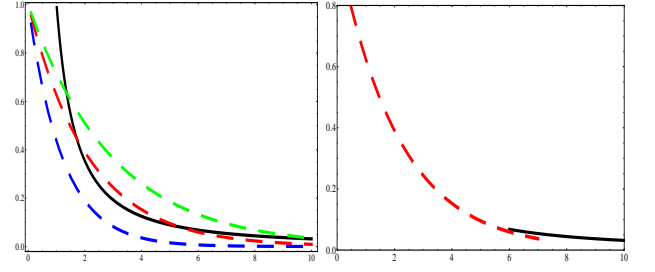


FIG. 6: Color online. In both panels, function $x^{-1.5}$ is shown by bold black line. Function b^{-x} is shown by dashed lines of various colors for $b = 1.4; 1.6$ and 2.3

$E_k > E_n$ in the long run. However, for some combinations of parameters and in some finite domains in k -space, the opposite relation can take place, $E_k < E_n$; the spectra E_k and E_n might be quite close and even coincide for some k (see Fig.6, left panel). Main characteristics allowing to distinguish between kinetic and dynamic cascades which can be easily observed in experimental data are summarized in the Table below.

Property	E_k	E_n
coherent phases	no	yes
dependence on the initial conditions	no	yes
local interactions	yes	no
existence of inertial interval	yes	not important

As some of the initial energy goes into P-modes not taking part in connections within the cascading cluster and zero-frequency mode transfers energy into k -spectrum via interactions of the form (8), phases become stochastic, 3-wave interactions with big enough resonance width appear and kinetic regime can be developed (shown in the Fig.6, right panel).

This scenario has been confirmed in laboratory experiments with parametrically excited capillary waves [18], the container shaken at frequencies from 0.5 to 3500 Hz. Energy contained in a zero-frequency band and a dynamic cascade are observed; they contain total energy E_{tot} of the system at lower forcing. Kinetic cascade occurs first at frequencies about 220 Hz and its energy grows (with increase of the forcing frequency) from $0.01 \cdot E_{tot}$ to $0.23 \cdot E_{tot}$, while energy contained in the dynamic cascade decreases from $0.82 \cdot E_{tot}$ to $0.46 \cdot E_{tot}$.

The understanding of differences between dynamic and kinetic cascades is of the utmost importance for correct interpretation of the experimental observations. Thus, in [1] weak turbulence of capillary waves in Helium has been studied and the formation of a local maximum of the wave-spectrum near a viscous cut-off was observed (under periodic driving force) and correctly attributed to the discrete regime (interactions are non-local). On the

other hand, "in the inertial range dependence of the peak amplitudes on frequency is described well by a power law function $I_\omega \sim \omega^{-m}$ with the index $m \approx 3.7$. This is in agreement with the weak turbulence theory which gives the value $m = 21/6$ " ([1], p.032001-3). As $21/6=3.5$, the observed and predicted indexes differ by about 6%. It would be worth to check phase coherence in this data in order to understand whether this discrepancy is due to the available accuracy of measurements or while in fact a dynamic cascade is observed and not a kinetic one.

5. Conclusions.

- In the system of weakly nonlinear capillary waves three substantially different turbulent regimes can occur: discrete, kinetic and mesoscopic.

Discrete regime can be observed in the form of frozen turbulence (distinct modes keeping their initial energies, energy flux is absent), or as a resonance clustering (a set of distinct modes dynamically exchanging energies among themselves). Irrotational capillary waves with dispersion function $\omega \sim k^{3/2}$ demonstrate fluxless modes, "there is virtually no energy absorption associated with high-wavenumbers damping in this case" ([15], p.107). On the contrary, rotational capillary waves have dispersion function $\omega(k) = -\frac{\Omega}{2} + \sqrt{\sigma|k|^3 + \frac{\Omega^2}{4}}$ with constant non-zero vorticity Ω , and their discrete regime is governed by resonance clustering, [4]. The necessary and sufficient condition for discrete regime to occur is small nonlinearity, **I**.

In *kinetic regime* energy transport is characterized by power spectra of energy (1), it might be observed only if the conditions **I–VI** take place.

In *mesoscopic regime* energy transport is realized by a dynamic cascade according to (10).

- Direct dynamic cascade is triggered by 4-wave interactions of the form (8), i.e. by the presence of a zero-frequency mode with non-zero energy. The fact that 4-wave resonances play substantial role in the time evolution of a system of weakly nonlinear capillary waves is confirmed by laboratory measurements in parametrically driven capillary waves, [16].

- In general, if dispersion function $\omega(\mathbf{k})$ has decay type, this only means that 3-wave resonance conditions

$$\omega(\mathbf{k}_1) + \omega(\mathbf{k}_2) = \omega(\mathbf{k}_3), \quad \mathbf{k}_1 + \mathbf{k}_2 = \mathbf{k}_3 \quad (19)$$

may have *some solutions*. This does not necessary mean that these solutions possess the properties **I–VI**. In particular, if $\omega(\mathbf{k}) \sim k^\gamma$, $\gamma > 1$, then both properties formulated in Sec.2.3 hold and the geometry of resonances

can be outlined in terms of resonance curves similar to those shown in Fig. 5.

Acknowledgements. The authors are grateful to M. Shats and S. Nazarenko for fruitful discussions. E.K. acknowledges the support of the Austrian Science Foundation (FWF) under the project P20164-N18 "Discrete resonances in nonlinear wave systems". A.K. acknowledges the support of AMS, Linz.

* Electronic address: lena@risc.uni-linz.ac.at

- [1] Abdurakhimov, L.V., M.Yu Brazhnikov, G.V. Kolmakov and A.A. Levchenko. *J. Physics: Conference Series* **150**: 032001 (2009).
- [2] Bustamante, M.D., and E. Kartashova. *EPL*, **85**: 34002 (2009).
- [3] Connaughton, C., S.V. Nazarenko and A.C. Newell. *Physica D* **184**: 86 (2003).
- [4] Constantin, A., and E. Kartashova. *EPL*, **86**: 29001 (2009).
- [5] Hasselmann, K. *Fluid Mech.*, **30**: 737 (1967).
- [6] Kartashova, E. *Physica D*, **46**: 43 (1990).
- [7] Kartashova, E. *JETP Lett.* **83**(7): 341 (2006).
- [8] Kartashova, E. *Europhys. Lett.* **87**: 44001 (2009).
- [9] Kartashova, E. *Nonlinear Resonance Analysis* (Cambridge University Press, 2010)
- [10] Kartashova, E, and V. S. L'vov. *EPL*, **83**: 50012 (2008).
- [11] Landau, L. D., and E. M. Lifshitz. *Mechanics (Course of Theoretical Physics, Vol. 1)* Pergamon Press, 2003
- [12] Melde, F. *Annalen der Physik und Chemie* **2**, **109**: 193 (1859); Anderson, P.W., and H. Suhl. *Phys. Rev.* **100**: 1788 (1955); Oraevsky, V.N., and R.Z. Sagdeev. *Zh. Tekh. Fiz.* **32**: 1291 (1962); [Sov. Phys. Tech. Phys. **7**: 955 (1963)]; Benjamin, T.B., and J.E. Feir. *Fluid Mech.*, **27**: 417 (1967); and others.
- [13] Punzmann, H., M. G. Shats and H. Xia. *Phys. Rev. Lett.* **103**: 064502 (2009).
- [14] Pushkarev, A. N. *Eur. J. Mech. – B/Fluids* **18**(3): 345 (1999).
- [15] Pushkarev, A.N., and Zakharov, V.E., 1999. *Physica D* **135**: 98.
- [16] Shats, M., H. Punzmann and H. Xia. *Phys. Rev. Lett.* **104**: 104503 (2010).
- [17] Verheest, F. *J. Math. Phys.* **29**: 2197 (1988).
- [18] Xia, H., M.G. Shats and H. Punzmann. Submitted to *EPL* (2010).
- [19] Zakharov, V. E., and N. N. Filonenko. *J. Appl. Mech. Tech. Phys.* **4**: 500 (1967).
- [20] Zakharov, V. E., A. O. Korotkevich, A. N. Pushkarev and A. I. Dyachenko. *JETP Lett.* **82**: 487 (2005).
- [21] Zakharov, V.E., V.S. L'vov and G. Falkovich. *Kolmogorov Spectra of Turbulence* (Springer, 1992).